Formations with a Mission: Stable Coordination of Vehicle Group Maneuvers

Petter Ögren*
petter@math.kth.se
Optimization and Systems Theory
Royal Institute of Technology
SE-100 44 Stockholm, Sweden

Edward Fiorelli and Naomi Ehrich Leonard†
eddie@princeton.edu, naomi@princeton.edu
Mechanical and Aerospace Engineering
Princeton University
Princeton, NJ 08544, USA

Abstract

In this paper we present a stable coordination strategy for vehicle formation missions that involve group translation, rotation, expansion and contraction. The underlying coordination framework uses artificial potentials and virtual leaders. Symmetry in the framework is exploited to partially decouple the mission control problem into a formation management subproblem and a maneuver management subproblem. The designed dynamics of the virtual leaders play a key role in both subproblems: the direction of motion of the virtual leaders is designed to satisfy the mission while the speed of the virtual leaders is designed to ensure stability and convergence properties of the formation. The latter is guaranteed by regulating the virtual leader speed according to a feedback measurement of an appropriate formation error function. The coordination strategy is illustrated in the context of adaptive gradient climbing missions.

1 Introduction

The main contribution of this paper is a method and proof for stably coordinating a group of vehicles to cooperatively perform a mission. Gradient climbing and adaptive sampling in a given region of the environment are examples of missions for which coordinated vehicle networks are expected to outperform current approaches (see, for example, [4] on adaptive ocean sampling networks). This expectation is motivated in part by the success of animal aggregations in searching their environment. Fish schools, for instance, are remarkably effective and efficient at finding the densest source of food, and biologists have developed a number of models for the traffic rules that govern their successful cooperative behavior (see, for example, [7, 11, 12, 13] and references therein). Coordinating control laws that are designed to produce the emergent behavior observed in biology for gradient climbing are described in [1, 2].

*This research was sponsored by the Swedish Foundation for Strategic Research through its Center for Autonomous Systems at KTH.

†This research was supported in part by the Office of Naval Research under grants N00014-98-1-0649 and N00014-01-1-0526, by the National Science Foundation under grant CCR–9980058 and by the Air Force Office of Scientific Research under grant F49620-01-1-0382.

Adaptive sampling problems refer to those in which the main objective is to efficiently gather data from the environment. The vehicle formation serves as a reconfigurable sensor array. Adaptation in this context might mean, for example, that the resolution of this sensor array adapts to the environment; the resolution increases (i.e., the vehicles form a tighter group) when there is considerable local variation in the measurements and decreases (i.e., a looser group) when there is little variation in measurements across the group.

In this paper we present a control strategy and a Lyapunov-based stability proof for translation, rotation, expansion and contraction of a vehicle formation. These then form the basic elements for missions. In this paper, we focus on gradient climbing missions with environment-driven group contraction and expansion.

We use as a setup for the construction and maintenance of vehicle formations the framework presented in [9]. This framework uses artificial potentials and virtual leaders. Virtual leaders are moving reference points that are used to herd the vehicle group and to enforce a desired group geometry. Artificial potentials define interaction forces between pairs of neighboring vehicles and between virtual leaders and nearby vehicles. The framework leads to decentralized control designs in which each vehicle responds to its local environment. No ordering of vehicles is necessary and this provides robustness to a vehicle failure.

In [9] the dynamics of the virtual leaders are independent of the behavior of the formation. This keeps the rules relatively simple. However, the independence becomes a problem in circumstances in which the formation cannot keep up with the virtual leaders. Following [10], we introduce in this paper virtual leader dynamics that are driven by a feedback error associated with the formation. Roughly speaking, we constrain motion of the virtual leaders in the event that the formation is not keeping up so that we can guarantee stability and convergence.

The stability properties of the formation (without feedback-driven virtual leader dynamics) were proved in [9] using Lyapunov's direct method. In this paper, by incorporating the magnitude of that same Lyapunov function as a feedback into the speed control of the virtual leaders, we are able to extend the stability results to the moving formation. We guarantee an upper bound on the Lyapunov function as well as convergence to the desired final state.

Our stabilized motion results go beyond those in [10] where motion of the virtual leader (and thus the formation) was limited to translation. Here we exploit the symmetry in the framework of [9] to extend the notion of virtual leader motion (and thus formation motion) to formation rotation and formation contraction and expansion. The idea is to consider a web of virtual leaders that move together like a rigid body. The motion of the virtual body is described by a position vector, an orientation matrix and a scale factor that characterizes the size and spacing of the web. Stabilized motion then includes the translation, orientation and scale factor variables so that the formation can be made to stably translate, rotate, expand and contract.

We push the framework even further to enable formation missions. Of particular interest are those missions that benefit not just from a translating formation but also from a formation that can perform a desired rotation and/or expansion and contraction (e.g., gradient climbing with adaptive spacing). To do so we use the remaining freedom in the virtual leader dynamics, that is, we prescribe the direction of the virtual leader variables (position, orientation and scale factor). The problems of maintaining a formation during virtual leader motion and controlling the motion of the virtual leaders to successfully perform a mission are partially decoupled in this framework.

Formation maintenance is guaranteed independent of the direction of the virtual leaders. This eases the problem of designing the mission control law since the formation error is bounded. We prove convergence in the case of gradient climbing missions.

There are a number of researchers who use artificial potentials and/or virtual leaders as part of a multi-agent control scheme (see, for example, references in [9]). Translation, rotation and expansion of a group is treated in [14] using a similar notion of a virtual rigid body called a virtual structure which has dynamics dependent on a formation error function. However, the formation control laws and the dynamics of the virtual structure differ from those presented here. For example, an ordering of vehicles is imposed in [14]. Gradient climbing with a vehicle network is also a topic of growing interest in the literature (see, for example, [5] and [2] and references therein), although adaptive expansion and contraction in this context is not addressed in these papers. In [3], the authors use Voronoi diagrams and information about a known environment to design control laws for a vehicle network to optimize sensor coverage.

The remainder of this paper is organized as follows. In §2, we review the formation framework of [9] based on artificial potentials and virtual leaders. Formation motion is introduced in §3 and the partially decoupled problems of formation stabilization and mission control are described. Formation stabilization is addressed in §4 followed by a simulation example for a group rotation in §5. Gradient climbing missions with adaptive formation spacing are treated in §6.

2 Artificial Potentials, Virtual Leaders and Symmetry

In this section we describe the underlying framework for decentralized formation control based on artificial potentials and virtual leaders. The framework follows that presented in [9] (with some variation in notation). Each vehicle in the group is modelled as a point mass with fully actuated dynamics. Extension to underactuated systems is possible. For example, in [8], the authors consider the dynamics of an off-axis point on a nonholonomic robot and use feedback linearization to transform the resulting system dynamics into fully actuated double integrator equations of motion.

Let the position with respect to an inertial frame of the ith vehicle in a group of N vehicles be given by a vector $x_i \in \mathbb{R}^l$, $i = 1, \ldots, N$ where $l = 1, 2$ or 3 as shown in Figure 1. The control force on the ith vehicle is given by $u_i \in \mathbb{R}^l$. Since we assume full actuation, the dynamics can be written for $i = 1, \ldots, N$ as

$$\ddot{x}_i = u_i.$$

We introduce a web of M reference points called virtual leaders and define the position of the kth virtual leader with respect to the inertial frame to be $b_k \in \mathbb{R}^l$, for $k = 1, \ldots, M$. Assume that the virtual leaders are connected, i.e., let them form a virtual body. The position vector from the origin of the inertial frame to the center of mass of the virtual body is denote $r \in \mathbb{R}^l$ as shown in Figure 1. In [9] the virtual leaders move with constant velocity. In this section we specialize to the case in which all virtual leaders are at rest. Motion of the virtual leaders will be introduced in §3.

Let $x_{ij} = x_i - x_j \in \mathbb{R}^l$ and $h_{ik} = x_i - b_k \in \mathbb{R}^l$. Between every pair of vehicles i and j we define an artificial potential $V_I(x_{ij})$ which depends on the distance between the ith and jth vehicles. Similarly, between every vehicle i and every virtual leader k we define an artificial potential $V_h(h_{ik})$ which depends on the distance between the ith vehicle and kth virtual leader.

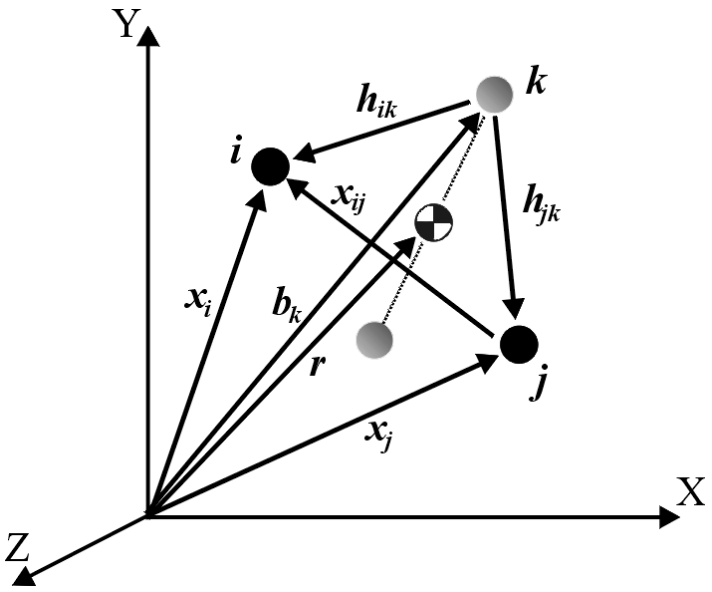

Figure 1: Notation for framework. Solid circles are vehicles and shaded circles are virtual leaders.

The control law u_i is defined as minus the gradient of the sum of these potentials plus a linear damping term:

$$\begin{aligned} u_i &= -\sum_{j\neq i}^{N} \nabla_{x_i} V_I(x_{ij}) - \sum_{k=1}^{M} \nabla_{x_i} V_h(h_{ik}) - K\dot{x}_i \qquad (2.1) \\ &= -\sum_{j\neq i}^{N} \frac{f_I(x_{ij})}{\|x_{ij}\|} x_{ij} - \sum_{k=1}^{M} \frac{f_h(h_{ik})}{\|h_{ik}\|} h_{ik} - K\dot{x}_i \end{aligned}$$

where K is a positive definite matrix.

We consider the form of potential V_I that yields a force that is repelling when a pair of vehicles is too close, i.e., when $\|x_{ij}\| < d_0$, attracting when the vehicles are too far, i.e., when $\|x_{ij}\| > d_0$ and zero when the vehicles are very far apart $\|x_{ij}\| \geq d_1 > d_0$, where d_0 and d_1 are constant design parameters. The potential V_h is designed similarly with possibly different design parameters h_0 and h_1 (among others). Typical forms for f_I and f_h are shown in Figure 2.

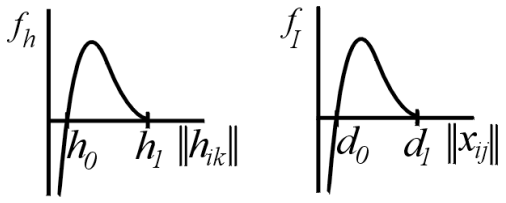

Figure 2: Representative control forces derived from artificial potentials.

Note that each vehicle uses exactly the same control law and is influenced only by near neighbor vehicles, i.e., those within a distance d_1, and nearby virtual leaders, i.e., those within a distance h_1.

The global minimum of the sum of all the artificial potentials consists of a configuration in which neighboring vehicles are spaced a distance d_0 from one another and a distance h_0 from neighboring virtual leaders.

The global minimum will not in general be unique. Since any vehicle can play any role in the network, any permutation of vehicles in a given configuration that corresponds to a global minimum will also be a global minimum. Further, because the potentials only depend upon relative distance, there may be rotational symmetry and therefore a continuous family of global minimizing solutions. This rotational symmetry can, if desired, be broken with additional virtual leaders. For example, Figure 3(a) shows two solutions in the S^1 family of solutions in the case of two vehicles and one virtual leader in 2D. In Figure 3(b) a second virtual leader is added which breaks the S^1 symmetry and fixes the orientation of the global minimum.

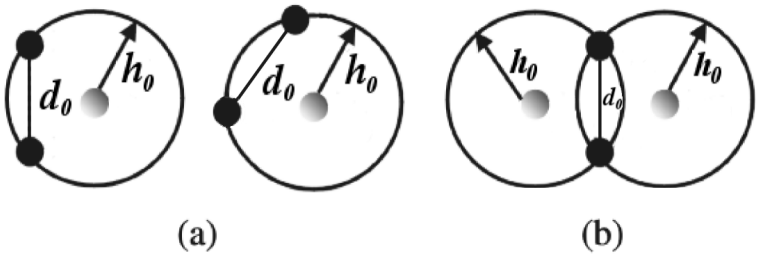

Figure 3: Equilibrium solutions for a formation in 2D with two vehicles. (a) With one virtual leader there is S^1 symmetry and a family of solutions. (b) With two virtual leaders the S^1 symmetry can be broken and the orientation of the group fixed.

We remark that it is sometimes of interest to have the option of breaking symmetry or not. Breaking symmetry by introducing additional virtual leaders can be useful for enforcing an orientation, but it may mean increased input energy for the individual vehicles. Under certain circumstances, it may not be feasible to provide such input energy and instead more practical to settle for a group shape and spacing without a prescribed group orientation. This was the case in an implementation of this control strategy for maintaining a uniform density of stratospheric balloons over the Northern Hemisphere [6]. These balloons have very limited control authority as compared with the magnitude of the winds in the stratosphere and so minimum energy use is critical.

The state of the vehicle group is $x = (x_1, \ldots, x_N, \dot{x}_1, \ldots, \dot{x}_N)$. In [9], local asymptotic stability of $x = x_{eq}$ corresponding to the vehicles at rest at the global minimum of the sum of the artificial potentials is proved with the Lyapunov function

$$V(x) = \frac{1}{2}\sum_{i=1}^{N}\left(\dot{x}_i \cdot \dot{x}_i + \sum_{j\neq i}^{N} V_I(x_{ij}) + 2\sum_{k=1}^{M} V_h(h_{ik})\right). \tag{2.2}$$

3 Formation Motion: Translation, Rotation, Expansion and Contraction

In this section we introduce motion of the formation by prescribing motion of the virtual leader body. This motion can include group translation, rotation, expansion and contraction. By parametrizing

the motion by the scalar variable s, we enable a decoupling of the problem of formation stabilization from the problem of formation maneuvering and mission control. In §4 we prescribe the dynamics ds/dt which depend on a feedback of a formation error, and we prove convergence properties of the formation. In §6 we prescribe the direction of the virtual leader motion, e.g., dr/ds, for gradient climbing and prove convergence properties of the virtual leaders to the source of the gradient field.

3.1 Translation and Rotation

The stability proof of [9] is invariant with respect to $SE(l)$, $l = 2, 3$ ($\mathbb{R}$ in the case $l = 1$) symmetries of the virtual leader body. Specifically, this means that given the positions b_k of the virtual leaders, every set of virtual leader positions

$$b'_k = Rb_k + r, \quad k = 1, \ldots, m$$

where $(R, r) \in (SO(l) \times \mathbb{R}^l) = SE(l)$, $l = 2, 3$ also works in the proof. This can be viewed as fixing the positions of the virtual leaders with respect to a "virtual body frame" and then moving the "virtual body" around in $SE(l)$.

Let $\bar{b}_k = b_k(s_s) - r(s_s)$, $k = 1, \ldots, m$, be the initial position of the kth virtual leader with respect to a virtual body frame oriented as the inertial frame but with origin at the virtual body center of mass. A trajectory in $SE(l)$ paramaterized by s is defined by $(R(s), r(s)) \in SE(l)$, $\forall s \in [s_s, s_f]$ such that

$$b_k(s) = R(s)\bar{b}_k + r(s).$$

Note that $R(s_s)$ is the $l \times l$ identity matrix.

3.2 Expansion and Contraction

For expansion and contraction we observe that the stability proof is still valid when we scale all distances between the virtual leaders and all distance parameters (d_i, h_i), $i = 0, 1$, by a factor $k(s) \in \mathbb{R}$. Incorporating this into the framework yields:

$$\begin{aligned} b_k(s) &= k(s)R(s)\bar{b}_k + r(s) \\ h_i(s) &= k(s)h_i \\ d_i(s) &= k(s)d_i, \end{aligned} \tag{3.3}$$

where $R(s)$ governs rotation, $r(s)$ translation and $k(s)$ expansion and/or contraction.

3.3 Retained Symmetries

As discussed in §2, it may be desirable to keep certain symmetries while controlling the formation. This can be accomplished by allowing the vehicles to influence the virtual leader dynamics. For instance, to keep the translational symmetry but break the rotational symmetry one can let $r(t)$ evolve according to dynamics with forces, derived from the artificial potentials, that the vehicles exert on the virtual leaders. These forces are equal in magnitude and opposite in direction to the forces the virtual leaders exert on the vehicles. For example, let m be the total mass of the virtual

body (if each virtual leader has unit mass then $m = M$). Then, we could set

$$\ddot{r} = -\frac{1}{m}\sum_{k=1}^{M}\sum_{i=1}^{N}\nabla_{b_k}V_h(h_{ik})$$

At the same time $R(s)$ would be made to evolve along a prescribed trajectory according to the dynamics of s.

Analogously, to keep the rotational symmetry and break the translational symmetry, one would let $R(t)$ evolve according to dynamics given by the moments, associated with forces derived from artificial potentials, that the vehicles exert on the virtual body. For example, suppose that $\mathbb{I} \in \mathbb{R}^{3\times 3}$ is the body-fixed inertia matrix for the virtual body about its center of mass, and let Ω denote the angular velocity of the virtual body with respect to the virtual body fixed frame. Then, we could set

$$\begin{aligned}\dot{R} &= R\hat{\Omega}\\ \mathbb{I}\dot{\Omega} &= \mathbb{I}\Omega\times\Omega - R^T\sum_{k=1}^{M}\sum_{i=1}^{N}\left((b_k - r)\times\nabla_{b_k}V_h(h_{ik})\right),\end{aligned}$$

where $\hat{\Omega}z = \Omega \times z$ for $z \in \mathbb{R}^3$. At the same time, $r(s)$ would be made to evolve along a prescribed trajectory according to the dynamics of s.

To prove stability in this case, one would add to the Lyapunov function the rotational and/or translational kinetic energies of the virtual leaders.

3.4 Mission Trajectories

A third option, apart from prescribed trajectories and free variables, would be to let translation, rotation, expansion and contraction evolve with feedback from sensors on the vehicles to carry out a mission such as gradient climbing. This would result in an augmented state space for the system given by (x, s, r, R, k). However, it is only the directions and not the magnitude of the virtual body vector fields that we can influence since ds/dt will already be prescribed to enforce formation stability. To see this decoupling of the mission control problem from the formation stabilization problem, note that the total vector fields for the virtual body motion can be expressed as

$$\dot{r} = \frac{dr}{ds}\dot{s}, \quad \dot{R} = \frac{dR}{ds}\dot{s}, \quad \dot{k} = \frac{dk}{ds}\dot{s}.$$

The prescription of $\dot{s}$, given in §4, controls the speed of the virtual body in order to guarantee formation stability and convergence properties. For the mission control problem, we design the directions

$$\frac{dR}{ds}, \ \frac{dr}{ds}, \ \frac{dk}{ds}.$$

In §6 we choose rules for directions and prove convergence in gradient climbing problems.

4 Speed of Traversal and Formation Stabilization

We now explore how fast we can move along a trajectory while staying within some estimated subset of the region of attraction. In the next theorem we prove that traversing the trajectory

$r(s), R(s), k(s)$ from $s = s_s$ to $s = s_f$ with the speed governed by equation (4.4) below will allow the formation to converge to the final destination while always remaining within the region of attraction, formulated as an upper bound V_U on the Lyapunov function $V(x, s)$. Here we will be interested in the Lyapunov function $V(x, s)$ that extends the Lyapunov function $V(x)$ given by equation (2.2) where b_k, d_i and h_i are replaced with $b_k(s)$, $d_i(s)$ and $h_i(s)$ according to (3.3).

4.1 Convergence and Boundedness

Theorem 4.1 (Convergence and Boundedness) *Let $V(x, s)$ be a Lyapunov function for every fixed choice of s with $V(x_{eq}(s), s) = 0$. Let V_U be a desired upper bound on the value of this Lyapunov function such that the set $\{x : V(x, s) \leq V_U\}$ is bounded. Let v_0 be a nominal desired speed for the formation. Let $\dot{s}$ be given by*

$$\dot{s} = \min \left\{ v_0,\ h(V(x,s)) + \frac{-\left(\frac{\partial V}{\partial x}\right)^T \dot{x}}{\delta + |\frac{\partial V}{\partial s}|} \left(\frac{\delta + V_U}{\delta + V(x,s)} \right) \right\} \tag{4.4}$$

with the addition that $\dot{s} = 0$ at the endpoint, $s = s_f$. Here $h : \mathbb{R}^+ \to \mathbb{R}^+$ has compact support within ($V < V_U/2$) and $h(0) > 0$. Then, the system is stable and asymptotically converges to $(x, s) = (x_{eq}(s_f), s_f)$ with $V(x, s) \leq V_U$ throughout.

Proof: **Boundedness** We directly have

$$\dot{V} = \left(\frac{\partial V}{\partial x}\right)^T \dot{x} + \frac{\partial V}{\partial s}\dot{s}(s,x)$$

$$\leq \left(\frac{\partial V}{\partial x}\right)^T \dot{x} + \frac{\partial V}{\partial s}\left(\frac{-(\frac{\partial V}{\partial x})^T \dot{x}}{\delta + |\frac{\partial V}{\partial s}|} \left(\frac{\delta + V_U}{\delta + V(s,x)} \right) + h(V(s,x)) \right).$$

Now, assume that $V(s(t_0), x(t_0)) \geq V_U$. This gives

$$h(V(s,x)) = 0, \qquad \frac{\delta + V_U}{\delta + V(s(t_0), x(t_0))} \leq 1,$$

$$\frac{\frac{\partial V(s(t_0),x(t_0))}{\partial s}}{\left(\delta + \left|\frac{\partial V(s(t_0),x(t_0))}{\partial s}\right|\right)} \leq 1, \qquad \left(\frac{\partial V(s(t_0), x(t_0))}{\partial x}\right)^T \dot{x}(t_0) \leq 0.$$

Thus

$$\dot{V} \leq \left(\frac{\partial V}{\partial x}\right)^T \dot{x} + \left(\frac{-(\frac{\partial V}{\partial x})^T \dot{x}}{1} 1 + 0 \right) = 0.$$

Therefore, if $V(s, x) \geq V_U$ then $\dot{V}(s, x) \leq 0$ along trajectories. Thus $V(s(t), x(t)) \leq V_U$ for all $t \geq t_0$ if $V(s(t_0), x(t_0)) \leq V_U$.

Asymptotic Stability

Let the extended state of the system be $(x, s) \in \mathbb{R}^n$, $n = 2N + 1$, and

$$\begin{aligned} \Omega_c &= \{(x,s) \in \mathbb{R}^n : s \in [s_s, s_f], V(x,s) \leq V_U\} \\ S &= \{(x,s) \in \Omega_c : \dot{s} = 0\}. \end{aligned}$$

Since $\dot{s} \geq 0$ and $s \in [s_s, s_f]$, the limit $s_0 = \lim_{t\to\infty} s(t)$ exists. By the boundedness property above, Ω_c is invariant and bounded. Thus, on Ω_c the ω-limit set L exists, is invariant and $(x, s) \to L \subset \Omega_c$. For $(x_L, s_L) \in L$ we must have $s_L = s_0$ and therefore $L \subset S$. We will now show that $\{(x_{eq}(s_f), s_f)\}$ is the largest invariant set in S and therefore $(x, s) \to \{(x_{eq}(s_f), s_f)\} = L$.

$\dot{s} = 0$ implies that $V(x, s)$ is a Lyapunov function with respect to x (since s is fixed). Therefore, every trajectory candidate approaches $x_{eq}(s)$, where $V(x_{eq}(s), s) = 0$. But this implies (by the choice of $\dot{s}$ in equation (4.4)) that $\dot{s} > 0$ (due to the h term, unless $s = s_f$ where the trajectory is completed and we let s halt). Therefore, $\{(x_{eq}(s_f), s_f)\}$ is the only invariant set in S. Thus, $(x, s) \to (x_{eq}(s_f), s_f)$ and the system is asymptotically stable. ∎

Remark 4.1 *A typical choice of $h(V)$ is*

$$h(V) = \begin{cases} \frac{1}{2}v_0 \left(1 + \cos\left(\pi \frac{2}{V_U} V\right)\right) & \text{if } |V| \leq \frac{V_U}{2} \\ 0 & \text{if } |V| > \frac{V_U}{2} \end{cases}$$

As can be seen it fulfills $h(0) = v_0 > 0$ guaranteeing asymptotic stability and giving $\dot{s} = v_0$ at $V = 0$ (never more because of the 'min'). Its support is limited to $|V| \leq \frac{V_U}{2}$ thus not affecting the $V \leq V_U$ property.

Remark 4.2 *If the Lyapunov function V is locally positive definite and decresent and $-\dot{V}$ is locally positive definite, then one can find a class $\mathcal{K}$ function σ such that*

$$\frac{-\left(\frac{\partial V}{\partial x}\right)^T \dot{x}}{\sigma(V(x, s))} \geq 1 \ , \to \infty \text{ as } V \to 0.$$

In this case stronger results can be proved, as shown in [10].

5 Simulation: Formation Rotation

Simulation of a two-vehicle planar rotation using two virtual leaders is presented in this section. To effect rotation about the center of mass of the virtual body, we parameterize a trajectory in $SO(2)$ by s with $\dot{s}$ dynamics prescribed by equation (4.4).

In this example, the two virtual leaders comprise the virtual body, and the distance between the two virtual leaders is chosen to be $2\sqrt{h_0^2 - d_0^2/4}$. The center of mass of the virtual body is fixed at the origin of the inertial frame, i.e., we take $r = 0 \in \mathbb{R}^2$. The simulation is started with the two virtual leaders in a line along the horizontal as shown in Figure 4(a). Initially, the two vehicles are in the stable configuration corresponding to the global minimum of the sum of the artificial potentials, i.e., they sit at a distance d_0 from one another and a distance h_0 from each of the virtual leaders, see Figure 4(a).

The objective of the rotation is to produce the formation shown in Figure 4(b). This is achieved by rotating the virtual body by 90°. The path of the virtual body is counterclockwise rotation $R(s) \in SO(2)$, equivalently $\theta(s) = s \in S^1$, where s goes from $s = s_s = 0$, to $s = s_f = \pi/2$. The nominal desired speed v_0 was chosen to be $v_0 = .3$ rad/s. Once the virtual leaders have rotated about the virtual center of mass by 90°, s is halted. The vehicles should then converge on the

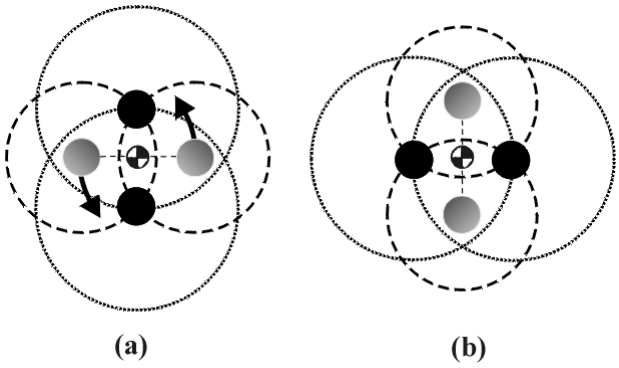

Figure 4: Formation rotation. Solid circles are vehicles and shaded circles are virtual leaders. The dotted circle around each vehicle has radius d_0 while the dashed circle around each virtual leader has radius h_0. a) Formation initially at global minimum of total potential. b) Formation after rotation by 90°.

new equilibrium configuration corresponding to the global minimum of the sum of the artificial potentials. This is the formation shown in Figure 4(b).

The control for each vehicle is given by equation (2.1) and is composed of the sum of the gradient of artificial potentials V_h and V_I in addition to a damping force $-K\dot{x}_i$. The artificial potentials used in this simulation are given by

$$V_I = \begin{cases} \alpha_I \left(\ln(x_{ij}) + \frac{d_0}{x_{ij}} \right) & 0 < x_{ij} < d_1 \\ \alpha_I \left(\ln(d_1) + \frac{d_0}{d_1} \right) & x_{ij} \geq d_1 \end{cases} \tag{5.5}$$

$$V_h = \begin{cases} \alpha_h \left(\ln(h_{ik}) + \frac{h_0}{h_{ik}} \right) & 0 < h_{ik} < h_1 \\ \alpha_h \left(\ln(h_1) + \frac{h_0}{h_1} \right) & h_{ik} \geq h_1. \end{cases} \tag{5.6}$$

These yield forces of the form shown in Figure 2.

The equations of motion were integrated in MATLAB for 20 seconds with parameters choices of $\alpha_I = 1$ N-m, $\alpha_h = 10$ N-m, $d_0 = 2\sqrt{2}$ m, $d_1 = 10$ m, $h_0 = 2$ m and $h_1 = 10$ m. The damping coefficient K was taken to be the $K = 3I$ kg/s, where I is the identity matrix.

The Lyapunov function $V(x, s)$ used in the $\dot{s}$ dynamics is the Lyapunov function $V(x)$ given by (2.2) extended to include the s-dependence of $h_{ik} = x_i(t) - b_k(s(t))$. This Lyapunov function is also modified by subtracting a constant so that $V(x_{eq}(s), s) = 0$. The upper bound V_U on $V(x, s)$ is chosen to be $V_U = 0.2$ N-m in the simulation. Figure 5 shows the evolution of the Lyapunov function (the formation error function) during the controlled rotation of the two-vehicle formation. The dashed line is corresponds to $V(x, s) = V_U$. Initially, $V(x, s) = 0$ since we start the vehicle at the equilibrium configuration for the initial virtual body orientation. During the rotation, $V(x, s)$ increases, but as expected $V(x, s) \leq V_U$ throughout.

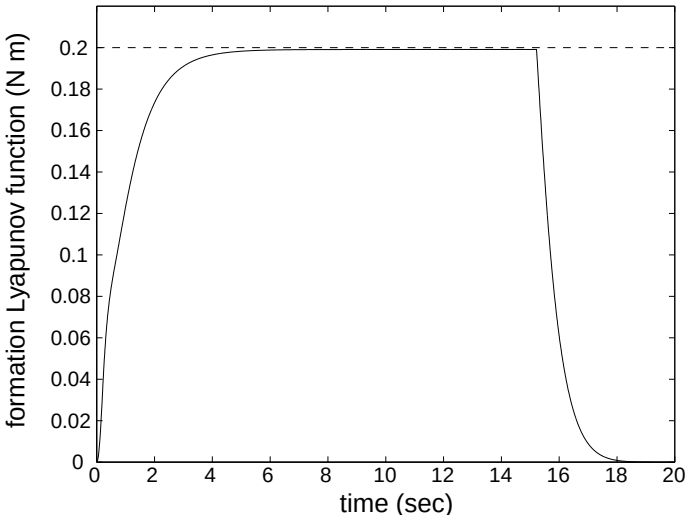

Figure 5: Formation function evolution for controlled group rotation.

6 Formation Mission: Gradient Climbing

One application in which formation motion and group expansion can be especially useful is that of tracking a source of pollution, a heat source or a mineral plume in the sea. Gradient climbing is an intuitive approach to solving this kind of problem. In the framework of this paper, the virtual body is directed to climb the gradient based on the measurements from the vehicles. The vehicles move with the virtual body and therefore climb the gradient as well. There are numerous options for how much and what kind of data is passed from the vehicles to the computer that will compute the gradient climb (or descent) algorithm that drives the virtual leaders. In this section we consider two possibilities in two-dimensional space.

In the first case, we assume that each vehicle measures the field (e.g., temperature) T at its current position and makes this information available for the calculation of the gradient at the position of the center of mass of the virtual body r. In the second case we let each (ith) vehicle use its history of measurements of T and approximate on its own the gradient of T at its position x_i. Assuming these gradient calculations can be communicated, they can be used to compute the gradient of T at r. In the following we investigate algorithms for directing the position vector r and the scaling variable k, the latter for adaptation of the spacing of the vehicles in the group.

Consider the first case in which each vehicle communicates its current measurement of T. Suppose we have three vehicles (in, for example, a triangular-shaped formation about the virtual body center of mass). Define $T_i = T(x_i)$, $\Delta x_{ij} = \|x_{ij}\| = \|x_i - x_j\|$ and $e_{ij} = (x_j - x_i)/\Delta x_{ij}$. Assume that e_{12} and e_{13} are linearly independent unit vectors (so that the matrix $(\, e_{12} \; e_{13} \,)$ invertible). A first-order estimate ∇T_e of the gradient of T at r is given by

$$\nabla T_e \, (\, e_{12} \; e_{13} \,) = \left(\begin{array}{cc} \frac{T_2 - T_1}{\Delta x_{21}} & \frac{T_3 - T_1}{\Delta x_{32}} \end{array} \right)$$

$$\Rightarrow \nabla T_e = \left(\begin{array}{cc} \frac{T_2 - T_1}{\Delta x_{21}} & \frac{T_3 - T_1}{\Delta x_{32}} \end{array} \right) (\, e_{12} \; e_{13} \,)^{-1}$$

Then, we set $\frac{dr}{ds} = \nabla T_e$ and the formation will move in the direction of the steepest increase of T.

Expansion of the formation can be used to improve the quality of the estimate by adjusting Δx_{ij} as a function of the variation of T in space. For instance, one would desire a tighter formation where T varies greatly for increased measurement resolution. Alternatively, where the variation in T is small over a large area, it may be best to expand the formation for more effective tracking.

Given a desired inter-vehicle distance Δ_d, let k evolve according to

$$\frac{dk}{ds} = -a(kd_0 - \Delta_d),$$

with $a > 0$ a scalar constant and d_0 the inter-vehicle equilibrium distance defined by the potential V_I, see Figure 2. In the following lemma, we derive a rule for choosing Δ_d.

Lemma 6.1 (Minimizing Error Bound) *Consider four vehicles moving in a square formation. Define the position of one of the four vehicles as $z = (x, y)$. Let the estimate of the gradient of T at $z = (x, y)$ be*

$$\begin{aligned}\nabla T_m(x,y) = &\left(\frac{1}{2}\frac{T_m(x+\Delta x,y)-T_m(x,y)}{\Delta x}+\frac{1}{2}\frac{T_m(x+\Delta x,y+\Delta y)-T_m(x,y+\Delta y)}{\Delta x},\right.\\ &\left.\frac{1}{2}\frac{T_m(x,y+\Delta y)-T_m(x,y)}{\Delta y}+\frac{1}{2}\frac{T_m(x+\Delta x,y+\Delta y)-T_m(x+\Delta x,y)}{\Delta y}\right),\end{aligned}$$

where $\Delta x = \Delta y = \Delta$ is the inter-vehicle distance (i.e., the length of the edge of the square), $T_m = T + d$ is the measurement of the field T and $|d| \le \epsilon$ is a disturbance. Then, the following inequality holds (ignoring higher order terms):

$$||\nabla T_m - \nabla T||^2 \le ((T_{xx}+T_{xy})^2 + (T_{yy}+T_{xy})^2)\frac{\Delta^2}{4} + |T_{xx}+2T_{xy}+T_{yy}|\frac{2\epsilon}{2} + 2(\frac{2\epsilon}{\Delta})^2,$$

where $T_x = \frac{\partial T}{\partial x}(x, y)$, $T_{xx} = \frac{\partial T_x}{\partial x}(x, y)$, etc. Furthermore, this bound is minimized by choosing

$$\Delta_d^2 = \frac{4\sqrt{2}\epsilon}{\sqrt{(T_{xx}+T_{xy})^2 + (T_{yy}+T_{xy})^2}}.$$

Proof: Using $T_m = T + d$ we get

$$\begin{aligned}\nabla T_m(z) = &\left(\frac{T(x+\Delta x,y)-T(x,y)+T(x+\Delta x,y+\Delta y)-T(x,y+\Delta y)}{2\Delta x}+\frac{\Delta d}{\Delta x},\right.\\ &\left.\frac{T(x,y+\Delta y)-T(x,y)+T(x+\Delta x,y+\Delta y)-T(x+\Delta x,y)}{2\Delta y}+\frac{\Delta d}{\Delta y}\right).\end{aligned}$$

By a two-dimensional Taylor series expansion we have $T(x+\Delta x, y+\Delta y) = T(x, y) + T_x(x, y)\Delta x + T_y(x, y)\Delta y + T_{xx}(x, y)\Delta x^2/2 + T_{yy}(x, y)\Delta y^2/2 + T_{xy}(x, y)\Delta x\Delta y + \mathcal{O}(\Delta^3)$. The true gradient is, of course, $\nabla T = (T_x, T_y)$ which gives the error

$$\begin{aligned}E &= \nabla T_m(x,y) - \nabla T(x,y)\\ &= \left(T_{xx}\Delta x/2 + T_{xy}\Delta y/2 + \mathcal{O}(\Delta^2) + \frac{\Delta d}{\Delta x},\ T_{yy}\Delta y/2 + T_{xy}\Delta x/2 + \mathcal{O}(\Delta^2) + \frac{\Delta d}{\Delta y}\right).\end{aligned}$$

Now let $\Delta x = \Delta y = \Delta$, ignore higher order terms and note that $|\Delta d| \leq 2\epsilon$. Then,

$$\begin{aligned} E &= \left(T_{xx}\frac{\Delta}{2} + T_{xy}\frac{\Delta}{2} + \frac{\Delta d}{\Delta}, T_{yy}\frac{\Delta}{2} + T_{xy}\frac{\Delta}{2} + \frac{\Delta d}{\Delta}\right) \\ ||E||^2 &= (T_{xx}+T_{xy})^2\frac{\Delta^2}{4} + (T_{xx}+T_{xy})\frac{\Delta d}{2} + \left(\frac{\Delta d}{\Delta}\right)^2 + (T_{yy}+T_{xy})^2\frac{\Delta^2}{4} + (T_{yy}+T_{xy})\frac{\Delta d}{2} + \left(\frac{\Delta d}{\Delta}\right)^2 \\ &\leq ((T_{xx}+T_{xy})^2 + (T_{yy}+T_{xy})^2)\frac{\Delta^2}{4} + |T_{xx}+2T_{xy}+T_{yy}|\frac{2\epsilon}{2} + 2\left(\frac{2\epsilon}{\Delta}\right)^2 = f(\Delta). \end{aligned}$$

Thus $f(\Delta)$ is a bound for the squared estimation error. Minimizing this bound we get

$$\begin{aligned} f'(\Delta) &= ((T_{xx}+T_{xy})^2 + (T_{yy}+T_{xy})^2)\frac{\Delta}{2} - 4\left(\frac{4\epsilon^2}{\Delta^3}\right) = 0 \\ \Delta_0^2 &= \frac{4\sqrt{2}\epsilon}{\sqrt{(T_{xx}+T_{xy})^2 + (T_{yy}+T_{xy})^2}} \end{aligned}$$

which is the distance above. ∎

Remark 6.1 *This verifies the intuitive notion of moving towards larger inter-vehicle distances when the second derivatives of T are small and the disturbances in the measurements, ϵ, are large.*

Remark 6.2 *Since estimations of second derivatives are very noise sensitive, these should either be filtered over time or estimated on the basis of some prior knowledge.*

Lemma 6.2 (Convergence of Gradient Climbing) *In the setting of Lemma 6.1 above, using the prescribed optimal distance Δ_d, assume that the virtual leader is anywhere inside the square of vehicles and moving in the direction $\frac{dr}{ds} = \nabla T_m(x,y)$. Suppose that the following inequality holds for the scalar field $T(x,y)$*

$$||\nabla T||^2 \geq 2\sqrt{2}\epsilon\sqrt{(T_{xx}+T_{xy})^2 + (T_{yy}+T_{xy})^2} + \epsilon|T_{xx}+2T_{xy}+T_{yy}|.$$

Then, the virtual leader, and thus the formation, will converge to a local optimum of T.

Proof: First note that the estimation T_m is symmetric with respect to the four measurements. The bound refers to the error from the true gradient in one of the corners, but this corner is arbitrary. Furthermore, the estimate is an even better approximation for the gradient of T at a point in the interior of the square. Thus, the bound holds for any position inside the square. Since $\frac{dr}{ds} = \nabla T_m(x,y)$ we can use $V(x,y) = -T(x,y)$ as a Lyapunov function. It is clear that we need $\nabla T \cdot \nabla T_m \geq 0$ for V to be decreasing and thus guaranteeing convergence. This means we need

$$\begin{aligned} \nabla T \cdot \nabla T_m &= \nabla T \cdot (\nabla T + E) \\ &= ||\nabla T||^2 + \nabla T \cdot E \\ &\geq ||\nabla T||^2 - ||\nabla T||||E|| \\ &= ||\nabla T||(||\nabla T|| - ||E||) \geq 0 \end{aligned}$$

Thus, we require $||\nabla T|| \geq ||E||$ and plugging Δ_d into the upper bound of $||E||$ we get

$$||\nabla T|| \geq 2\sqrt{2}\epsilon\sqrt{(T_{xx}+T_{xy})^2 + (T_{yy}+T_{xy})^2} + \epsilon|T_{xx}+2T_{xy}+T_{yy}|$$

which is the condition above. ∎

Remark 6.3 *If one incorporates deviations from the perfect square in the above analysis the calculations will get messier due to the loss of orthogonality and the fact that $\Delta x \neq \Delta y$. The above result is however a good rule of thumb.*

Alternatively, consider the situation where each vehicle can compute and communicate the gradient of T at its current position. In practice such information could be obtained from multiple sensors on each vehicle. In the case of a single sensor per vehicle, each vehicle could still compute the gradient of T projected in its direction of motion [1, 2]. In the following lemma, we propose an algorithm for gradient descent of a three-vehicle triangular formation in a quadratic gradient field $T(q) = \frac{1}{2}q^T P q$, $q \in \mathbb{R}^2$ and prove convergence to the minimum of this field.

Lemma 6.3 (Gradient Descent in Quadratic Field) *Consider three vehicles and a virtual leader with artificial potentials defined with global minimum corresponding to the vehicles in a triangular formation about the virtual leader. Let the control law be given by equation (2.1). Consider the gradient field $T(q) = \frac{1}{2}q^T P q$, $q \in \mathbb{R}^2$, where $P \in \mathbb{R}^{2\times 2}$ is positive definite. Let each (ith) vehicle be capable of measuring the local gradient, $\nabla T(x_i) = P x_i$. Define $r_i = x_i - r$. For each of the three vehicles, define a_i to be the area of the triangle with vertices coincident with the other two vehicles and virtual leader, i.e. $a_i = \frac{1}{2}||r_j \times r_k||$ for $i, j, k \in \{1, 2, 3\}$ and $i \neq j, i \neq k, j \neq k$. Additionally, let $a = \sum_{i=1}^{3} a_i$. If the virtual leader is given dynamics*

$$\dot{r} = \frac{dr}{ds}\dot{s}$$

with

$$\frac{dr}{ds} = -\sum_{i=1}^{3} \frac{a_i}{a} \nabla T(x_i)$$

and $\dot{s}$ given by equation (4.4) where $V(x, s)$ given by equation (2.2) with global minimum at zero, the formation will asymptotically converge to the minimum of T, i.e., r will converge to the origin and the formation will converge to the equilibrium at $s = s_f$. Further, $V(x, s) \leq V_U$ throughout.

Proof: Convergence of the virtual leader to the minimum of T can be proven with the Lyapunov function Φ given by

$$\Phi(r) = T(r) = \frac{1}{2} r^T P r.$$

We compute

$$\begin{aligned}
\dot{\Phi} \;=\; \nabla T(r) \cdot \dot{r} \;&=\; -\frac{\dot{s}}{a} \nabla T(r) \cdot \sum_{i=1}^{3} a_i \nabla T(x_i) \\
&=\; -\frac{\dot{s}}{a} P r \cdot \sum_{i=1}^{3} a_i P x_i \\
&=\; -\frac{\dot{s}}{a} P r \cdot \sum_{i=1}^{3} a_i P (r_i + r) \;=\; -\dot{s} ||Pr||^2 \leq 0
\end{aligned}$$

since $\sum_{i=1}^{3} a_i r_i = 0$. Boundedness and convergence of the formation Lyapunov function ($V(x, s) \leq V_U$) follows from Lemma 4.1. ∎

Remark 6.4 *The quantity* $\sum_{i=1}^{3} \frac{a_i}{a} \nabla T(x_i)$ *is essentially a first-order (linear) approximation of the gradient field at* r, $\nabla T(r)$. *Thus, for a quadratic field* T *the approximation is exact.*

Remark 6.5 *The result in Lemma 6.3 holds locally near the minimum of a more general gradient field when, near the minimum, the field can be approximated by a quadratic.*

References

[1] R. Bachmayer and N.E. Leonard. Experimental test-bed for multi-vehicle control, navigation and communication. In *Proc. 12th Int. Symposium on Unmanned Untethered Submersible Tech.*, Durham, NH, 2001.

[2] R. Bachmayer and N.E. Leonard. Vehicle networks for gradient descent in a sampled environment. Submitted, see http://www.princeton.edu/~ naomi, 2002.

[3] J. Cortés, S. Martínez, T. Karatas, and F. Bullo. Coverage control for mobile sensing networks: Variations on a theme. In *Proc. Mediterranean Conf. on Control and Automation*, 2002.

[4] T. B. Curtin, J. G. Bellingham, J. Catipovic, and D. Webb. Autonomous oceanographic sampling networks. *Oceanography*, 6:86–94, 1989.

[5] V. Gazi and K. Passino. Stability analysis of social foraging swarms. Preprint, February 2002.

[6] Global Aerospace Corporation. Constellation management–hemispherical network. http://www.gaerospace.com/publicPages/projectPages/StratCon/conMgtSims/hemisphericNetwork.html.

[7] D. Grünbaum. Schooling as a strategy for taxis in a noisy environment. *Evol. Ecol.*, pages 503–522, 1998.

[8] J. Lawton, B. Young, and R. Beard. A decentralized approach to elementary formation maneuvers. *IEEE Transactions on Robotics and Automation*, 2002. To appear.

[9] N.E. Leonard and E. Fiorelli. Virtual leaders, artificial potentials and coordinated control of groups. In *Proc. 40th IEEE Conference on Decision and Control*, pages 2968–2973, 2001.

[10] P. Ögren, M. Egerstedt, and X. Hu. A control Lyapunov function approach to multi-agent coordination. In *Proc. 40th IEEE Conference on Decision and Control*, pages 1150–1155, 2001.

[11] A. Okubo. Dynamical aspects of animal grouping: swarms, schools, flocks and herds. *Advances in Biophysics*, pages 1–94, 1985.

[12] J. K. Parrish and L. Edelstein-Keshet. From individuals to emergent properties: Complexity, pattern, evolutionary trade-offs in animal aggregation. In *Science*, pages 99–101, April 2 1999.

[13] J. K. Parrish and W. H. Hammer, editors. *Animal Groups in Three Dimensions.* Cambridge University Press, 1997.

[14] B.J. Young, R.W. Beard, and J.M. Kelsey. A control scheme for improving multi-vehicle formation maneuvers. In *Proc. American Control Conference*, pages 704–709, 2001.